
Article:
Nnakwo, K.C., Nwajioke, C.T., Chukwuneke, J.L. et al. (2024) Microstructure evolution in A356 alloy subjected to controlled heat treatment regimes processes. Discover Applied Sciences, 6 (10). 497. ISSN: 2523-3963

https://doi.org/10.1007/s42452-024-06143-2

Discover Applied Sciences

Research

Microstructure evolution in A356 alloy subjected to controlled heat treatment regimes processes

Kingsley C. Nnakwo[1] · Christian T. Nwajioke[1] · Jeremiah L. Chukwuneke[2] · Bonaventure C. Ugwuanyi[3,4] · Kennedy C. Ogbunaoffor[5] · Christopher C. Ozoh[6]

Received: 29 April 2024 / Accepted: 7 August 2024
Published online: 16 September 2024

Abstract
Aluminium–silicon alloys are highly regarded for their lightweight and unique mechanical properties, making them crucial for various industrial applications. Achieving optimal mechanical behavior in Al-Si-based alloys necessitates meticulous control over their microstructure. The research investigated the impacts of heat treatment regimes on the microstructure of A356 hypoeutectic alloys by light optical microscope (OM), scanning electron microscope (SEM), and energy dispersive spectroscope (EDS). The alloy, produced via stir-casting, underwent homogenization at 540 °C/5 h, one-step (200 °C for 0.5–8 h (T1)) and two-step (T2 (200 °C/0.5 h/180 °C/0.5–8 h)), and T2L (200 °C/0.5 h/160 °C/0.5–8 h)) aging processes. The findings revealed significant microstructural changes due to heat treatment. Homogenization reduced the average grain size of eutectic silicon by 20.5%. The T1 treatment increased the grain size and changed the grain morphology with prolonged aging, negatively impacting the mechanical properties. The T2 and T2L treatments resulted in finer, more uniform grain structures. The T2L treatment produced the finest eutectic silicon and the most uniform grain distribution, indicating the superior potential for mechanical performance. Overall, this study underscores the importance of tailored heat treatment regimes to optimize the microstructure and enhance the structural sensitive properties of Al-Si alloys, benefiting automotive and aerospace industries.

Article Highlights

- Significant Microstructural Refinement: Homogenization at 540 °C/5 h reduced the eutectic silicon grain size by 20.5%, from 4.4 µm to 3.5 µm, demonstrating adequate refinement of the alloy's microstructure.
- Impact of Aging Treatments: One-step aging at 200 °C increased grain size and changed grain morphology from rounded to dendritic, while two-step aging treatments showed varying degrees of grain refinement, with finer structures observed at lower secondary aging temperatures (160 °C).
- Optimization for Industrial Applications: The study emphasizes the importance of optimizing aging times to balance grain refinement, highlighting the potential for tailored alloy microstructure development to enhance performance in aerospace and automotive sectors.

✉ Kingsley C. Nnakwo, kc.nnakwo@unizik.edu.ng; Christian T. Nwajioke, stojix@yahoo.com; Jeremiah L. Chukwuneke, jl.chukwuneke@unizik.edu.ng; Bonaventure C. Ugwuanyi, bonaventure.ugwuanyi@esut.edu.ng; Kennedy C. Ogbunaoffor, chukwuemekakennedy@hotmail.com; Christopher C. Ozoh, chibuike.ozoh@futo.edu.ng | [1]Department of Metallurgical and Materials Engineering, Nnamdi Azikiwe University, Awka, Nigeria. [2]Department of Mechanical Engineering, Nnamdi Azikiwe University, Awka, Nigeria. [3]Department of Metallurgical and Materials Engineering, Enugu State University of Science and Technology, Agbani, Nigeria. [4]Material Science and Engineering, University of Sheffield, Sheffield, UK. [5]Department of Metallurgical and Materials Engineering, Akanu Ibiam Federal Polytechnic Unwana, Afikpo, Ebonyi, Nigeria. [6]Department of Metallurgical and Materials Engineering, Federal University of Technology, Owerri, Nigeria.

Keywords A356 hypereutectic alloy · Grain modification · Grain size · Grain morphology · α-Al matrix

1 Introduction

Aluminium–silicon (Al-Si) alloys stand out in materials science owing to their lightweight and unique mechanical properties, making them indispensable for various industrial applications [1–6]. Among these alloys, the Al-7Si-2 Mg-1Cu alloy system has attracted significant attention because of its favourable combination of mechanical strength and processability.

Previous studies have extensively explored various aspects of Al alloys, with emphasis on the impact of the characteristics of the Al-matrix and eutectic structure on the properties of the alloys. Shaha et al. [7] and Liu et al. [8] investigated the impact of V, Cu, Ti, and Fe on the microstructure of Al-Si alloys. Transition metal (TM) elements including Zr, V, and Ti promoted the formation of strengthening phases, leading to finer microstructures and improved mechanical properties [9–11]. Additionally, incorporating Fe-based amorphous alloys, Mg, and Sb resulted in significant reduction in the size of the α-Al matrix and eutectic silicon phases [12–14]. Various grain refinement techniques have been explored, including friction stir processing (FSP), warm rolling (WR), selective laser melting (SLM), and master alloys [15–18]. FSP and WR effectively disrupted the eutectic structure and reduced the porosity, leading to fine grain precipitation and a uniform dispersion of microstructural constituents. The incorporation of master alloys; Al5Ti1B and Al5Ti0.62C1.07La resulted in microstructural changes, improving the properties of the alloy [18, 19]. Grain refinement and modification strategies consistently induce high mechanical performance of Al alloys [18–30]. Liao et al. [31] and Wu et al. [32] obtained enhanced eutectic silicon characteristics in AlSiMg alloys through a controlled solidification process and 0.1 wt% (Zr and V) additions, respectively. These factors led to significant improvements in the mechanical performance of the alloys.

Several studies [9, 33–35] have investigated the effects of metallurgical processes including solution treatment, aging, and stress relief on the microstructure development in Al-Si alloys. Heat treatment enhances the α-Al matrix, eutectic silicon, and intermetallic phases characteristics. Recent studies [23, 36–42] have focused on optimizing processing parameters such as cooling rates, direct aging, and solution-treated and aging processes to achieve the desired microstructural characteristics for improving the mechanical performance of Al-Si. Zhang et al. [43] generated nanosized precipitates in an Er-doped Al7Si0.6 Mg alloy through a direct aging heat treatment process. Hwang et al. [44] reported the development of internal stress and its adverse impacts on the mechanical behavior of quenched Al–Si–Mg-based alloys. After direct aging treatment, the AlSi7Mg alloy demonstrated a poor strengthening effect due to the precipitation of coarse primary silicon. Park et al. [45] explored the microstructural characteristics of directly aged and T6-treated AlSiMg alloys. The research reported increases in the volume fraction of Si particles post heat treatment. Ming et al. [46] studied the grain characteristics of AlSiMg alloys annealed, directly aged, and T6 treated. The direct aged samples exhibited a discontinuous Al-Si network and nanosized Si particles, which became enlarged after annealing treatment. T6 treatment led to the precipitation of coarse eutectic silicon with irregular morphology. Wu et al. [47] demonstrated that deformation temperature and ratio significantly affected the microstructural characteristics of Al12.5Si0.6Mg0.1Ti alloys, with the deformation ratio having a greater effect on the dynamic recrystallization of the Mg_2Si phase.

Achieving optimal mechanical performance in Al-Si-based alloys requires careful control of their microstructure, particularly the α-Al matrix and eutectic silicon. The specific effects of heat treatment regimes on the refinement and modification of the α-Al matrix and eutectic structure of Al-7Si-2 Mg-1Cu alloys remain unclear. The research aimed to establish the impact of various heat treatment regimes on microstructural evolution, thereby contributing to a deeper understanding of the heat treatment parameters-microstructure interrelationship in Al-7Si-2 Mg-1Cu alloys. This study is crucial for metallurgy and materials engineering because it offers significant insights into how heat treatment regimes influence the α-Al matrix and eutectic silicon structure, including size and morphology. The two-step heat treatments and their effects on microstructure characteristics are novel, highlighting the benefits of complex heat treatment regimes in enhancing alloy performance, a topic less commonly addressed in existing research. These findings are crucial for industries such as automotive and aerospace, where fine-tuning the mechanical properties through controlled heat treatments can lead to superior component performance and longevity. This study underscores the importance of optimizing aging times and demonstrates the potential for tailored alloy microstructure development, distinguishing it from other research that typically focuses on more limited aspects of heat treatment effects.

While A356 alloy is a common material investigated under various thermal treatments, the impact of coarse and needle-like eutectic silicon in the mechanical performance of A356 alloys remains a challenge to scientific communities. Previous studies have focused on the use of master alloys [18–20] and various heat treatment processes like annealing,

normalizing, and single aging (T6) to promote eutectic silicon transformation into a spherical grain morphology for enhanced mechanical performance in service [15, 19, 33, 35, 43–46]. However, there is notably limited literature on the impact of multiple-step heat treatment regimes on A356 alloys. This study explored novel heat treatment processes: one-step and two-step heat treatment regimes (200 °C for 0.5 h, 200 °C for 0.5 h followed by 180 °C/0.5–8 h, and 200 °C for 0.5 h followed by 160 °C/0.5–8 h). The research analyzed how multiple-step heat treatment regimes affect the morphology, size, and distribution of the eutectic silicon phase in the alloy. It highlights the morphological transition of eutectic silicon from dendritic or rod-like forms to fine-rounded structures, particularly under the multiple-step heat treatment regime. The study's findings emphasize the potential for developing customized heat treatment protocols that can precisely modify the microstructure of A356 alloys. This approach provides significant advancements in processing techniques, optimizing the alloy's performance for specialized applications in various industries.

2 Experimental procedure

The stir-casting technique was employed in the A356 hypoeutectic alloy (Al-7wt%Si-2wt%Mg-1wt%Cu) development using high-grade aluminium, copper, silicon, and magnesium. The A356 alloy samples were cooled slowly to ambient temperature in the mold, and the elemental constituents were analyzed by X-ray fluorescence. The cast A356 alloy underwent homogenization at 540 °C/5 h and was water-cooled. The alloy underwent various heat treatment regimes presented in Fig. 1. T1 depicts a one-step heat treatment regime at 200 °C/ 0.5–8 h. T2 and T2L refer to two-step heat treatment regimes at 200 °C/0.5 h, followed by aging at 180 °C and 160 °C for 0.5–8 h, respectively. The microstructures were analyzed by light optical microscope (OM) and scanning electron microscope (SEM, EVO/NA10) with energy dispersive spectroscope (EDS), after undergoing pre-preparation including grinding (with 400, 600, 800, and 1200 µm grits silicon carbide papers), polishing (with alumina powder), and etching (with Keller's reagent; solution of iron (III) chloride, hydrochloric acid, and water). The grain size, morphology, and distribution were examined using the linear intercept method (LIM).

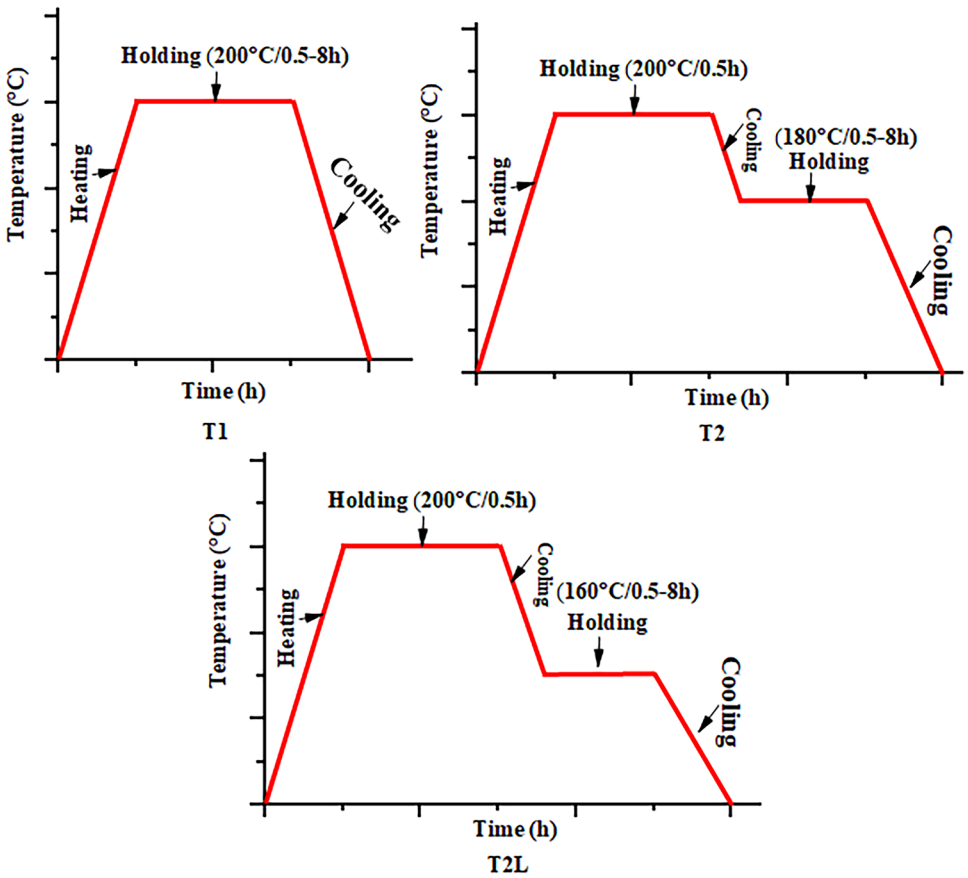

Fig. 1 Heat treatment regimes

3 Results and discussion

3.1 Results

The nominal composition of the as-cast Al-7Si-2 Mg-1Cu alloy was analyzed using X-ray fluorescence. Table 1 presents the results of the chemical constituents of the alloy. Figures 2–5 detail the impacts of multiple-step heat treatment regimes on the microstructures of the A356 alloy. Figure 2a, b depict the scanning electron microscopy (SEM) image and energy dispersive spectrum of the as-cast (AC) A356 alloy. Figure 2c, d reveal the microstructural features (SEM) and the elemental composition of the solution-treated and quenched (STQ) A356 alloy. The SEM images of the AC and STQ A356 alloy indicated changes in the microstructural features, revealing the impact of STQ on the microstructure of the A356 alloy. Figure 2e, f show the grain characteristics of the AC and STQ alloy, revealing the grain size, volume, and distributions. Figure 3 details the microstructural features (OM and SEM) of A356 subjected to one-step heat treatment regime (T1) at 200 °C for 0.5, 4, and 8 h after undergoing STQ. Figure 3e, f represent the elemental constituents of the T1 alloy. The images reveal different microstructural features compared with the AC and STQ, confirming the significant impact of T on the microscopic level. The OM and SEM images of A356 alloy subjected to a multiple-step heat treatment regime (T2; 200 °C for 0.5 h and 180 °C/0.5–8 h) presented in Fig. 4 reveal grain modification compared with the AC, STQ, and T1. Figure 4e, f depict the EDS and grain features of the T2. Figure 5 details the impact of a multiple-step heat treatment regime (T2L; 200 °C for 0.5 h and 160 °C/0.5–8 h) on the microstructure and grain characteristics of A356 alloy. The grains show different morphology and distributions compared with the AC, STQ, SA, and T2. Comparatively, T2 and T2L precipitated modified grains with elongated and rounded characteristics at 4 and 8 h, respectively. T1 precipitated networks of dendritic grains which grow in volume and size with aging time [48].

3.2 Discussion

The XRF analysis reveals elements including aluminium, silicon, magnesium, copper, iron, and titanium in the A356 alloy (Table 1).

Comparative analysis of OM and SEM microstructures of AC, STQ, T1, and multiple-step heat treated (T2 and T2L) A356 alloy demonstrates adequate grain refinement and modification after the multiple-step heat treatment regimes. The SEM microstructure of the AC A356 alloy consists of α-Al and eutectic silicon phases. The eutectic silicon exhibits coarse microstructural features with an average size of 8.84 µm. The EDS analysis reveals Al, Si, Cu, Mg, Ti, and Fe constituents in the as-cast alloy (Fig. 2b). The microstructure of STQ A356 alloy consists of finer grains of eutectic silicon at the microscopic level, as shown in Fig. 2c. The grain size decreased from 8.84 µm to 3.5 µm, indicating a 60.4% decrease compared to the as-cast A356 alloy. The SEM microstructure reveals a wide range of solid solution regions, indicative of increased dissolution of solutes in the aluminium matrix. Analysis of the precipitated phase reveals Al, Cu, Fe, C, and O as presented in the EDS spectrum (Fig. 2d).

Figure 3 shows the microstructural features of the A356 alloy subjected to a one-step heat treatment regime at 200 °C for 0.5 h (T1). The microstructure at 0.5 h aging time comprised sparsely distributed finer eutectic silicon with an average size of 3.7 µm. The eutectic silicon grows into networks of dendritic grains as the aging time increases to 4 h, as shown in Fig. 3b. The increase in size and volume of eutectic silicon is due to solute diffusion accompanying the aging process. Analysis of Fig. 3a–c reveals changes in grain morphology at the microscopic level compared with the AC and STQ alloy. The dendritic networks of eutectic silicon increased further at a longer aging time (8 h) with an average grain size of 4.32 µm. Prolonged aging time promotes precipitation of coarse grain, leading to poor mechanical performance of A356 alloy [46, 47]. The EDS analysis confirmed the presence of Al, Cu, O, Fe, and Cl as constituents.

Figures 4, 5 depict the microstructural features of A356 alloy subjected to multiple-step heat treatment regimes (T2 and T2L). The microstructures of T2 and T2L reveal changes in microstructure morphology compared with the AC, STQ, and T1 alloys at 4 and 8 h aging times. The eutectic silicon transformed from a needle-like shape to rounded patterns, as shown in Fig. 4c, b. The eutectic silicon morphological change to a spherical or rounded pattern is governed by the dissolution and sheroidization of eutectic silicon dendritic networks during thermal treatment [48]. The microstructure of T2 consists of a finer α-Al phase and short rod-like eutectic silicon with a grain size of 4.05 µm after

Table 1 Chemical constituents of the Al-7Si-2 Mg-1Cu alloys

Elements	Al	Si	Mg	Cu	Fe	Ti
Nominal composition (wt%)	89.80	6.50	2.15	0.9	0.3	0.2

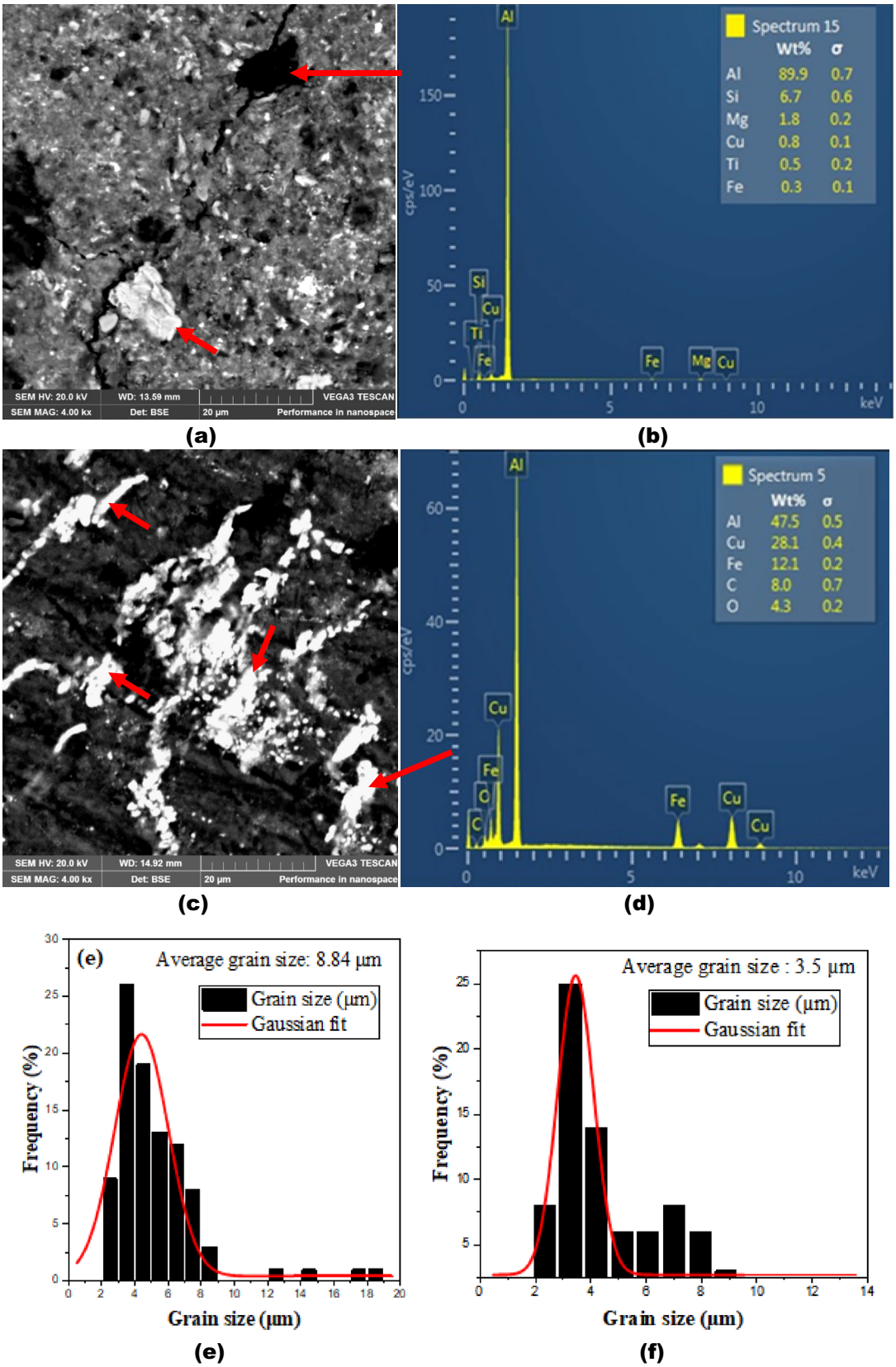

Fig. 2 SEM microstructures and EDS of A356 alloy (**a**, **b**) AC and (**c**, **d**) STQ. Grain distribution of A356 alloy (**e**) AC (**f**) STQ

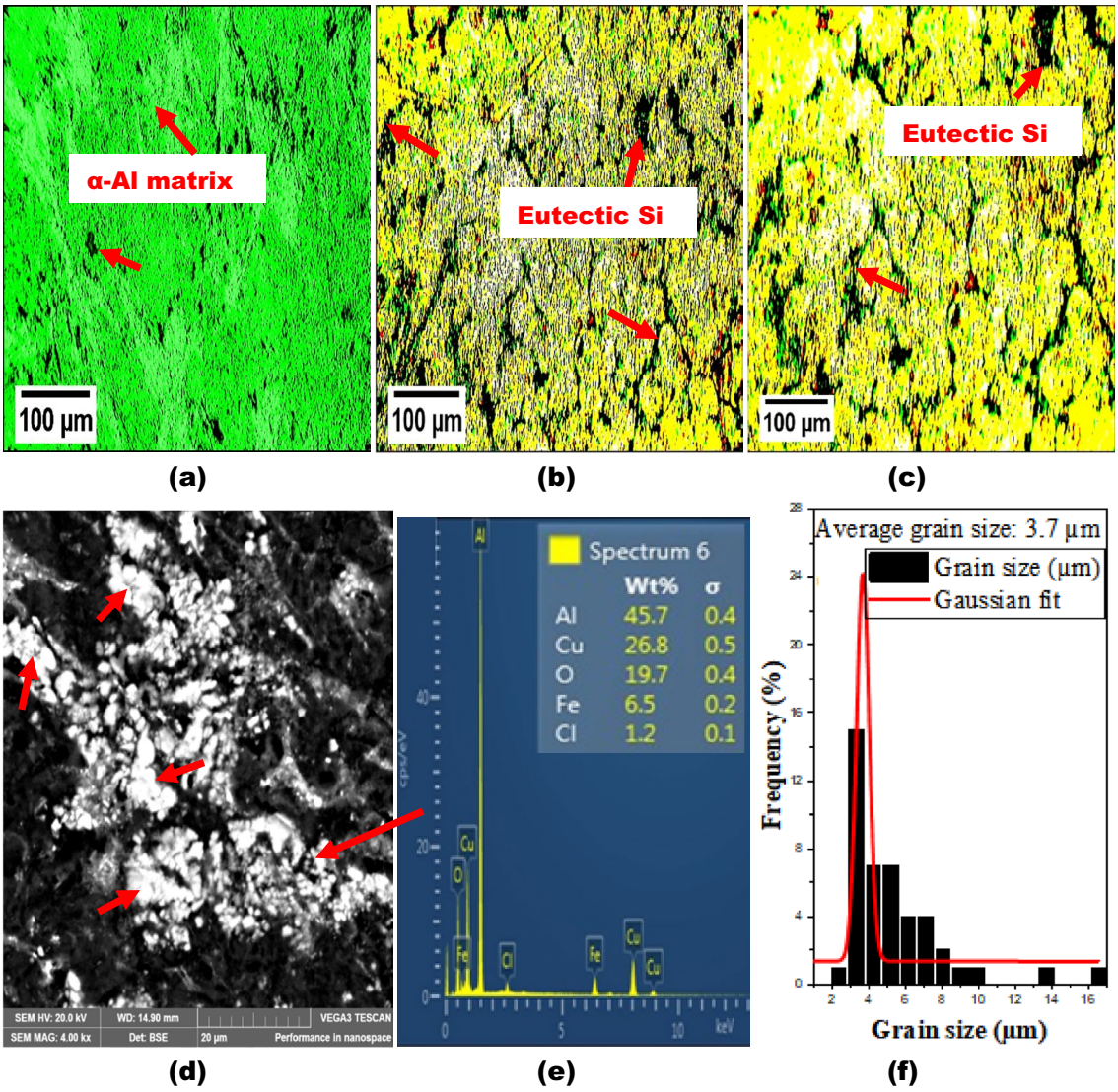

Fig. 3 OM microstructures of the A356 alloy subjected to T1 (**a**) 0.5 h, (**b**) 4 h, and (**c**) 8 h (**d**–**f**) SEM image, EDS spectrum and grain distribution curve of the A356 alloy aged at 200 °C for 0.5 h

0.5 h aging time. Increasing the aging time to 4 h led to a change in the eutectic silicon morphology from rod-like to rounded shape, with an average size of 4.69 µm. The morphology of the eutectic silicon changed further to elongated grains with an average grain size of 5.71 µm as the aging time increased to 8 h. The EDS spectrum identified Al, Cu, Fe, C, and O, as shown in Fig. 4e. The OM microstructure of the A356 alloy subjected to a multiple-step heat treatment regime (T2L; 200 °C/0.5 h/160 °C/0.5–8 h) consists of a dendritic network of eutectic silicon structure with an average grain size of 3.81 µm. The eutectic silicon stricture changed to a rounded structure at increasing aging time. The mechanical performance of A356 alloy is enhanced by transforming coarse needle-like eutectic silicon to short plate-like or rounded grains after T6 treatment [32, 48]. The precipitation rate and volume fraction of eutectic silicon increased with aging time [47]. The grain size distribution curves illustrate an even dispersion of grains within the aluminium matrix. Comparatively from the microscopic point, multi-step heat treatment regimes promote better grain modification at longer aging compared with the direct aging heat-treated A356 alloys (T6) [49, 50].

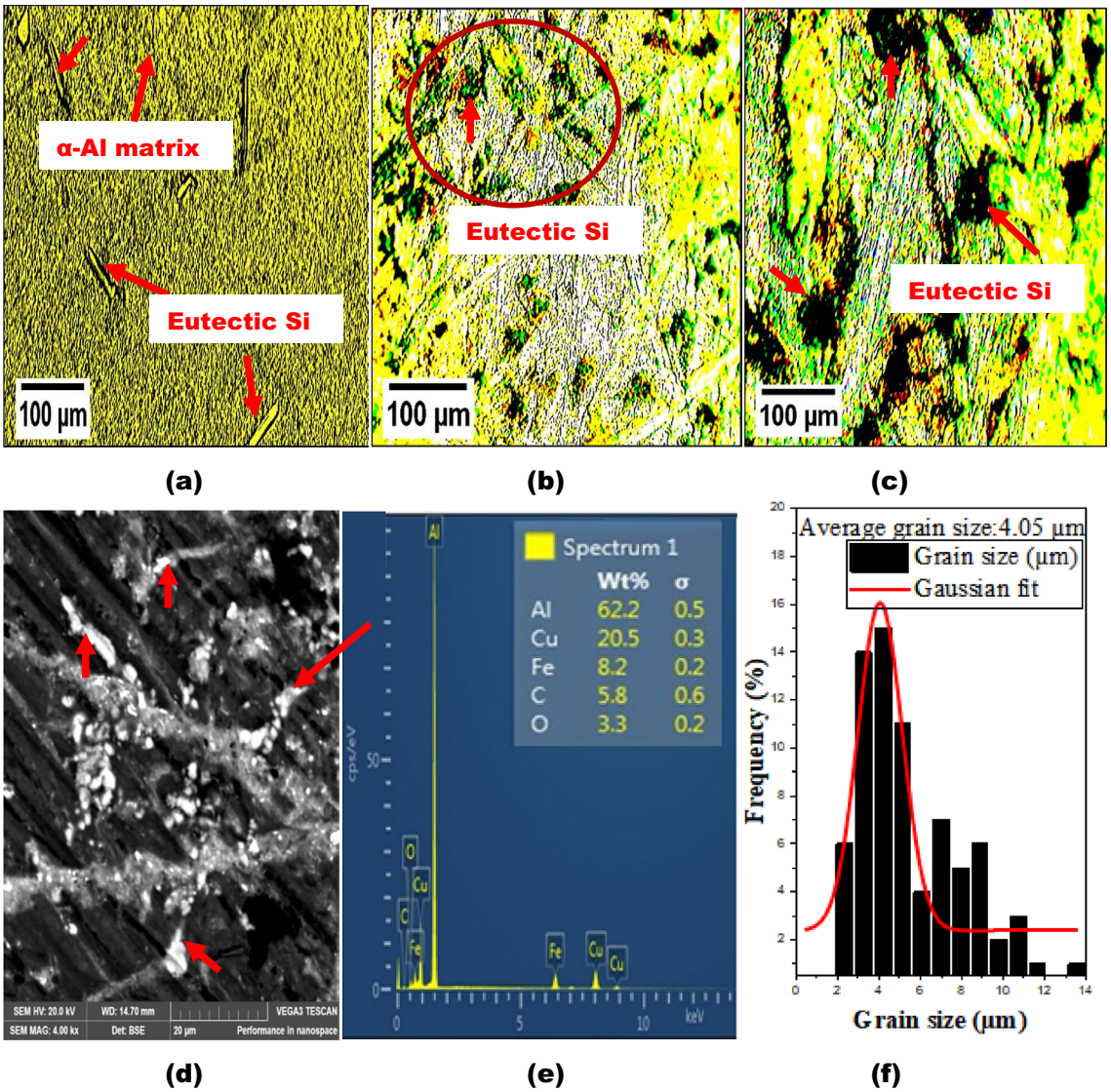

Fig. 4 OM microstructures of the A356 alloy subjected to a T2 (**a**) 0.5 h, (**b**) 4 h, and (**c**) 8 h. (**d**–**f**) SEM, EDS and grain distribution curve of the A356 alloy for 0.5 h

4 Conclusion

The research investigated the impact of heat treatment regimes on the microstructure of a stir-cast A356 hypoeutectic alloy. The study revealed significant changes in microstructure, after homogenization and subsequent aging treatments at different temperatures: T1 (200 °C/0.5–8 h), T2 (200 °C/0.5 and 180 °C/0.5–8 h), and T2L (200 °C/0.5 h and 160 °C/0.5–8 h). The findings are summarized below:

1. The controlled heat treatment regimes significantly influenced the grain characteristics of the A356 hypoeutectic alloy.
2. Homogenization at 540 °C for 5 h significantly reduced the average eutectic silicon size from 4.4 µm to 3.5 µm, indicating grain refinement.
3. T1, T2, and T2L treatment resulted in an increase in eutectic silicon size to 3.7 µm, 4.05 µm, and 3.81 µm, respectively, after 0.5 h of aging.
4. Morphological changes from dendritic or rod-like to fine-rounded eutectic silicon phases were observed at T2L with increasing aging time, indicating potential enhancements in the mechanical properties.

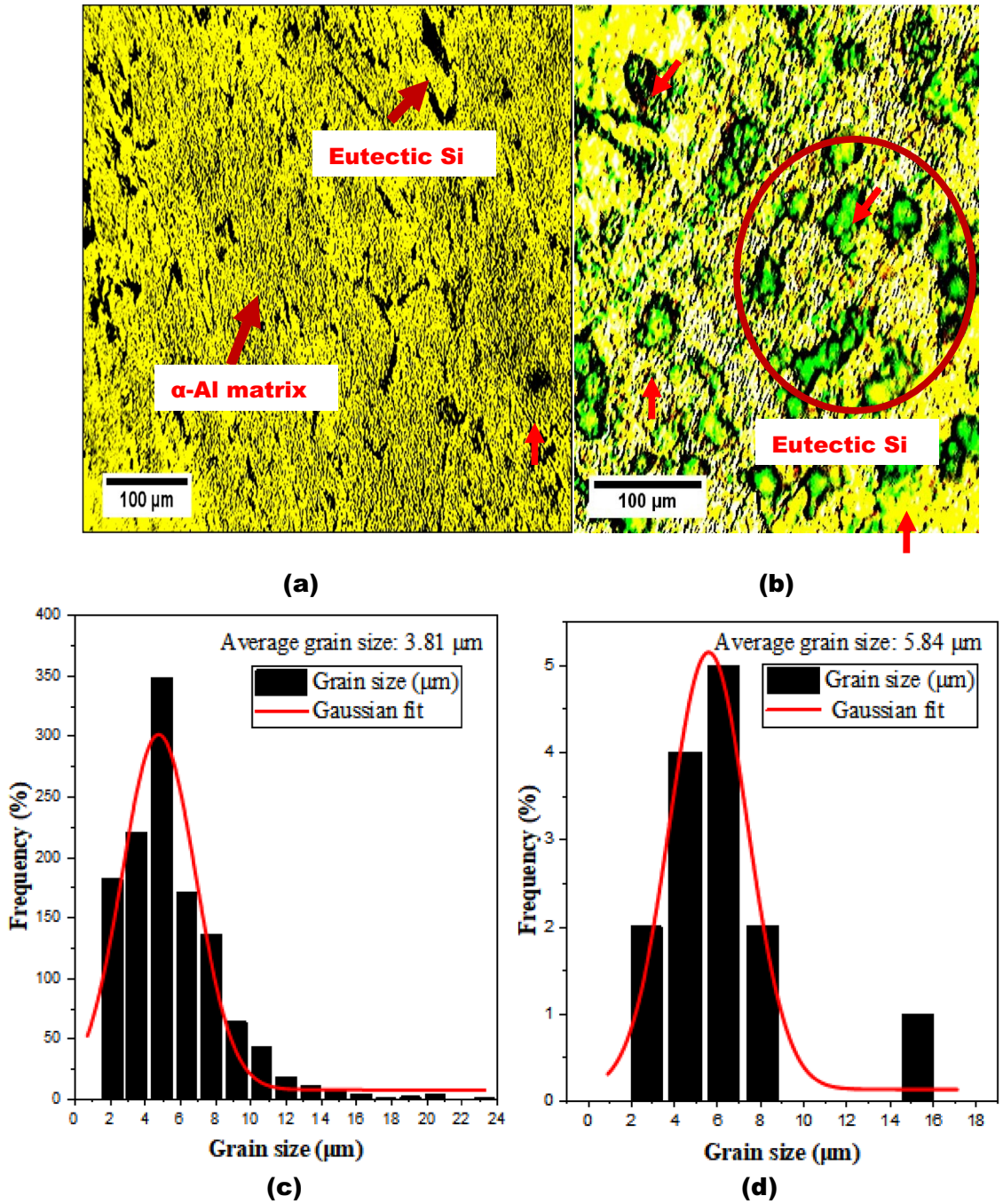

Fig. 5 OM microstructures of Al356 alloy subjected to a T2L for (**a**) 0.5 h (**B**) 8 h. Grain distribution curves (**c**) 0.5 h (**d**) 8 h

5. Prolonged aging leads to grain coarsening, decreasing the mechanical behavior of the alloy.
6. The findings highlight the potential for developing customized heat treatment protocols to enhance the performance of A356 alloys in automotive and aerospace industries.

Acknowledgements The authors appreciate the technical assistance of Dr. Kingsley C. Nnakwo for this research.

Author contributions Kingsley Chidi Nnakwo designed the alloy composition and the experimental route. Christian T. Nwajioke fabricated and analyzed the alloy samples. Kingsley Chidi Nnakwo and Jeremiah L. Chukwuneke supervised the research. Bonaventure C. Ugwuanyi Kennedy

Chukwuemeka Ogbunaoffor, and Christopher C. Ozoh contributed financially to the experiment. Kingsley Chidi Nnakwo wrote the first and final version of the manuscript, and all authors read and approved the final manuscript. Christopher C. Ozoh responded to the reviewer's comments.

Funding The authors have not disclosed any funding.

Data availability The data will be provided on request.

Declarations

Competing interests The authors declare no competing interests.

References

1. Nnakwo KC, Nnuka EE, Odo JU, Obiorah SM, Oghenekowho PA. Effect of magnesium and manganese on the secondary phase and mechanical properties of aluminium-4%copper alloy. Int J Eng Res Technol. 2014;3(8):1267–76.
2. Nnakwo KC, Odo JU, Ijomah AI. Mechanical characteristics of stir-cast Irvingia wombolu reinforced Al-4wt%Cu composite. Int J Novel Res Civil Struct Earth Sci. 2023;10(3):1–7.
3. Nnakwo KC, Odo JU, Ijomah AI. Reinforcing potential of Irvingia wombolu shell particulates in Al-2Nb-0.5Si eco-composite. Int J Novel Res Civil Struct Earth Sci. 2023;10(3):8–14.
4. Daniel-Mkpume CC, Okonkwo EG, Aigbodion VS, Offor PO, Nnakwo KC. Silica sand modified aluminium composite: an empirical study of the physical, mechanical and morphological properties. Mater Res Express. 2019;6: 076539. https://doi.org/10.1088/2053-1591/ab14c6.
5. Emeruwa OE, Nnakwo KC, Atuanya CU. Investigative study of the structure and mechanical behaviour of horse eye bean seed shell ash reinforced aluminium alloy matrix composite. Int J Sci Res Sci Eng Technol. 2017;3(5):8–13.
6. Odo JU, Nnakwo KC, Obiorah SMO, Mbah CN, Nwoye CI, Ifejika AC. Effect of iron removal on the structure and mechanical properties of aluminium-silicon alloys. Int J Sci Res Sci Eng Technol. 2015;1(6):555–62.
7. Shaha SK, Czerwinski F, Kasprzak W, Friedman J, Chen DL. Improving high-temperature tensile and low-cycle fatigue behavior of Al-Si-Cu-Mg Alloys through Micro-additions of Ti, V, and Zr. Metall Mater Trans A. 2015;46(7):3063–78.
8. Liu FZ, Qin J, Li Z, Yu CB, Zhu X, Nagaumi H, Zhang B. Precipitation of dispersoids in Al–Mg–Si alloys with Cu addition. J Mater Res Technol. 2021;14:3134–9.
9. Chen S, Liu K, Chen XG. Elevated-temperature low-cycle fatigue behaviors of Al-Si 356 and 319 foundry alloys. Minerals Metals Mater Series. 2019. https://doi.org/10.1007/978-3-030-05864-7_33.
10. Czerwinski F, Shaha SK, Kasprzak W, Friedman J, Chen DL. Effect of transition metals on thermal stability of Al-Si cast alloys. Front Mater Proces Applicat Res Technol. 2018. https://doi.org/10.1007/978-981-10-4819-7_25.
11. Wang M, Pang JC, Li SX, Zhang ZF. Low-cycle fatigue properties and life prediction of Al-Si piston alloy at elevated temperature. Mater Sci Eng A. 2017;704:480–92.
12. Dash SS, Li DJ, Zeng XQ, Li DY, Chen DL. Low-cycle fatigue behavior of Silafont®-36 automotive aluminum alloy: effect of negative strain ratio. Mater Sci Eng A. 2022;852: 143701. https://doi.org/10.1016/j.msea.2022.143701.
13. Dash SS, Li DJ, Zeng XQ, Li DY, Chen DL. Cyclic deformation behavior and fatigue life prediction of an automotive cast aluminum alloy: a new method of determining intrinsic fatigue toughness. Fatigue Fract Eng Mater Struct. 2022;45(3):725–38.
14. Liu TS, Qiu F, Shu SL, Kou SQ, Yang HY, Duan TT, Jiang QC. Multilevel microstructure control of cast Al–7.0Si–4.0Cu alloy with high strength–toughness synergy via micro-alloying combined with manipulation by in-situ nano-ceramics. J Mater Res Technol. 2022;21:3248–61.
15. Cheng W, Liu CY, Huang HF, Zhang L, Zhang B, Shi L. High strength and ductility of Al–Si–Mg alloys fabricated by deformation and heat treatment. Mater Charact. 2021;178:111278.
16. Yang KV, Rometsch PJ, Davies CHJ, Huang A, Wu X. Effect of heat treatment on the microstructure and anisotropy in mechanical properties of A357 alloy produced by selective laser melting. Mater Des. 2018;154:275–90.
17. Khalikova GR, Zakirova GR, Farkhutdinov AI, Korznikova EA, Trifonov VG. The structure and mechanical properties of the AK12D (Al–Si–Cu–Ni–Mg) aluminum alloy subjected to friction stir processing. Front Mater Technol. 2022;3(2):99–108.
18. Ding W, Xu C, Zhang H, Zhao W. Effects of Al-5Ti-0.62C-1.07La intermediate alloy on the microstructure and mechanical properties of A356 aluminium alloy. Mater Res Express. 2020. https://doi.org/10.1088/2053-1591/ab80ec.
19. Choudhary C, Sahoo KL, Keche AJ, Mandal D. Effect of ti addition on the microstructure and mechanical properties of hypo-eutectic and eutectic Al–Si alloys. Minerals Metals Mater Series. 2023. https://doi.org/10.1007/978-3-031-22532-1_63.
20. Liu X, Beausir B, Zhang Y, Gan W, Yuan H, Yu F, Esling C, Zhao X, Zuo L. Heat-treatment induced defect formation in α-Al matrix in Sr-modified eutectic Al–Si alloy. J Alloys Compd. 2018;730:208–18.

21. Liu M, Zheng R, Xiao W, Yu X, Peng Q, Ma C. Concurrent enhancement of strength and ductility for Al-Si binary alloy by refining Si phase to nanoscale. Mater Sci Eng A. 2019;751:303–10.
22. Liu TS, Zhao JR, Miao TJ, Han X, Zhang S, Qiu F. Comparison of in situ nanocrystals, Sr and nanocrystals + Sr manipulating microstructures and mechanical properties of eutectic Al–Si13.0–Cu5.0–(Ni2.0)–Mg0.6 alloy. J Mater Res Technol. 2020;9(4):7486–98.
23. de Albuquerque Sousa SM, de Gouveia GL, Spinelli JE. Evaluating grain size, dendritic scale, and tensile properties of a NbB-inoculated 6201 alloy using solidification rate. Mater Sci Eng A. 2022. https://doi.org/10.1016/j.msea.2022.142680.
24. Pereira CL, Gomes LF, Garcia A, Spinelli JE. Comparing the roles of Sb and Bi on microstructures and application properties of the Al-15% Si alloy. J Alloys Compd. 2021. https://doi.org/10.1016/j.jallcom.2021.160343.
25. Baganis A, Bouzouni M, Papaefthymiou S. Phase field simulation of aa6xxx aluminium alloys heat treatment. Metals. 2021;11(2):1–19.
26. Chen S, Liu K, Chen XG. Effect of Mo on elevated-temperature low-cycle fatigue behavior of Al-Si 356 cast alloy. Minerals, Metals and Materials Series. 2020. https://doi.org/10.1007/978-3-030-36408-3_37
27. Colombo M, Gariboldi E, Morri A. Er addition to Al-Si-Mg-based casting alloy: effects on microstructure, room and high temperature mechanical properties. J Alloys Compd. 2017;708:1234–44.
28. Deev V, Prusov E, Ri E, Prihodko O, Smetanyuk S, Chen X, Konovalov S. Effect of melt overheating on structure and mechanical properties of al-mg-si cast alloy. Metals. 2021;11(9):1353–65.
29. Derin S, Birol Y, Aybarc U. Effect of strontium addition on microstructure and mechanical properties of AlSi7Mg0.3 alloy. Int J Metalcast. 2017;11(4):688–95.
30. Hao J, Yu B, Bian J, Chen B, Wu H, Li W, Li Y, Li R. Calculation based on the formation of Mg2Si and its effect on the microstructure and properties of Al-Si alloys. Materials. 2021;14(21):6537.
31. Liao H, Wu Y, Chen H, Qian L. Divorced eutectic solidification in hypereutectic Al–Si alloys. Metall Mater Trans A. 2022;53(7):2346–50.
32. Wu Y, Liao H, Zhou K, Yang J. Effect of texture evolution on mechanical properties of near eutectic Al-Si-Mg alloy with minor addition of Zr/V during hot extrusion. Mater Des. 2014;57:416–20.
33. Wang M, Song B, Wei Q, Zhang Y, Shi Y. Effects of annealing on the microstructure and mechanical properties of selective laser melted AlSi7Mg alloy. Mater Sci Eng A. 2019;739:463–72.
34. Casati R, Vedani M. Aging response of an A357 Al alloy processed by selective laser melting. Adv Eng Mater. 2019. https://doi.org/10.1002/adem.201800406.
35. Guo B, Chang L, Dai J, Ding Y, Li R, Ding J, Li C, Tang Y, Xia X, Chen X, Song K, Liu Y. Effect of heat treatment on the microstructure and mechanical properties of Al–9Si–0.4Mg–0.1Cu alloy. Adv Eng Mater. 2022. https://doi.org/10.1002/adem.202200569.
36. Kleiven D, Ødegård OL, Laasonen K, Akola J. Atomistic simulations of early stage clusters in Al–Mg alloys. Acta Mater. 2019;166:484–92.
37. Li Y, Hu B, Liu B, Nie A, Gu Q, Wang J, Li Q. Insight into Si poisoning on grain refinement of Al-Si/Al-5Ti-B system. Acta Mater. 2020;187:51–65.
38. Nikanorov SP, Osipov VN, Regel LI. Structural and mechanical properties of directionally solidified Al-Si alloys. J Mater Eng Perform. 2019. https://doi.org/10.1007/s11665-019-04414-3.
39. Nowak M, Bolzoni L, Hari BN. Grain refinement of Al-Si alloys by Nb-B inoculation. Part I: concept development and effect on binary alloys. Mater Des. 2015;66:366–75.
40. Odinachi CC, Nnakwo KC, Nwoke VI, Nnuka EE. Effect of soaking time and quenching media on the structure and mechanical properties of Al-5.6wt%Zn2.5wt%Mg alloy. Int J Sci Res Sci Eng Technol. 2017;3(5):1–7.
41. Van Cauwenbergh P, Samaee V, Thijs L, Nejezchlebová J, Sedlák P, Iveković A, Vanmeensel K. Unravelling the multi-scale structure–property relationship of laser powder bed fusion processed and heat-treated AlSi10Mg. Sci Rep. 2021. https://doi.org/10.1038/s41598-021-85047-2.
42. Wei C, Guangxin W, Jieyu Z. Design and properties of Al-10Si-xZn-yMg alloy for hot dip coating. Surf Coat Technol. 2021;416:127–34.
43. Zhang B, Wei W, Shi W, Guo Y, Wen S, Wu X, Gao K, Rong L, Huang H, Nie Z. Effect of heat treatment on the microstructure and mechanical properties of Er-containing Al-7Si-06 Mg alloy by laser powder bed fusion. J Mater Res Technol. 2022;18:3073–84.
44. Hwang WJ, Bang GB, Choa SH. Effect of a stress relief heat treatment of AlSi7Mg and AlSi10Mg alloys on mechanical and electrical properties according to silicon precipitation. Metals Mater Int. 2023;29(5):1311–22.
45. Park TH, Baek MS, Hyer H, Sohn Y, Lee KA. Effect of direct aging on the microstructure and tensile properties of AlSi10Mg alloy manufactured by selective laser melting process. Mater Charact. 2021. https://doi.org/10.1016/j.matchar.2021.111113.
46. Ming X, Song D, Yu A, Tan H, Zhang Q, Zhang Z, Chen J, Lin X. Effect of heat treatment on microstructure, mechanical and thermal properties of selective laser melted AlSi7Mg alloy. J Alloys Compd. 2023. https://doi.org/10.1016/j.jallcom.2023.169278.
47. Wu Y, Liao H, Lü C. Dynamic precipitation and recrystallization in Al-125 wt%Si-0.6 wt%Mg-0.1 wt%Ti alloy during hot-rolling and their impacts on mechanical properties. J Alloys Compd. 2019;788:125–35.
48. Azimi H, Nourouzi S, Jamaati R. Effects of Ti particles and T6 heat treatment on the microstructure and mechanical properties of A356 alloy fabricated by compocasting. Mater Sci Eng A. 2021. https://doi.org/10.1016/j.msea.2021.141443.
49. Hadadzadeh A, Amirkhiz BS, Mohammadi M. Contribution of Mg2Si precipitates to the strength of direct metal laser sintered AlSi10Mg. Mater Sci Eng A. 2019;739:295–300.
50. Ikhmayies S. Phase diagrams of Al–Si system. Minerals Metals Mater Series. 2019:231–237.